Article:
Lovell, H, Livingstone, SJ, Boston, CM et al. (3 more authors) (2019) Complex kame belt morphology, stratigraphy and architecture. Earth Surface Processes and Landforms, 44 (13). pp. 2685-2702. ISSN 0197-9337

https://doi.org/10.1002/esp.4696

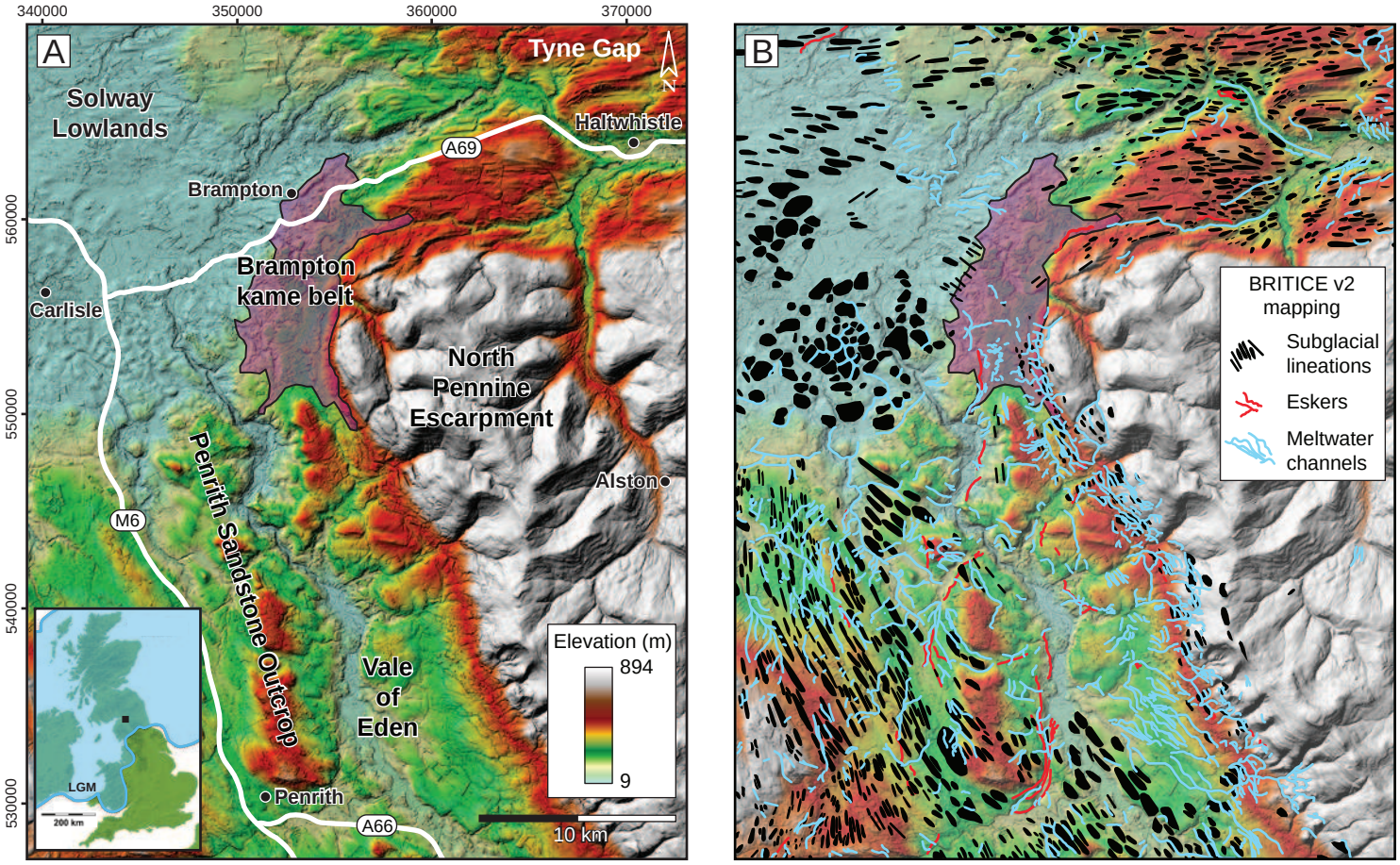
A
B
340000
350000
360000
370000
560000
550000
540000
530000
Tyne Gap
N
Solway
Lowlands
Haltwhistle
A69
Brampton
Brampton
kame belt
Carlisle
North
Pennine
Escarpment
Alston
M6
Penrith Sandstone Outcrop
Vale
of
Eden
Penrith
A66
LGM
200 km
Elevation (m)
894
9
10 km
BRITICE v2
mapping
Subglacial
lineations
Eskers
Meltwater
channels

Fig. 1

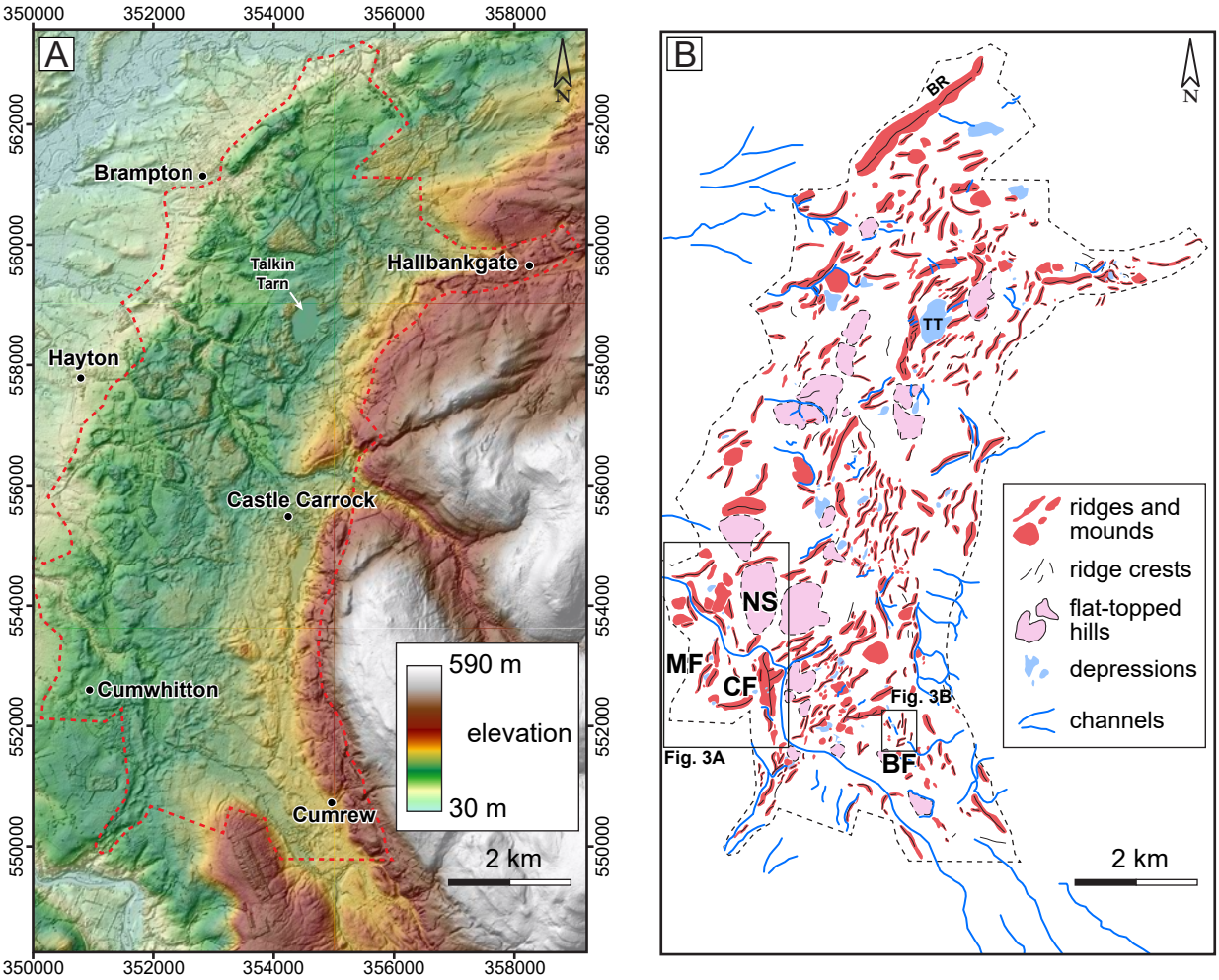

Figure 2 – (A) NEXTMap mosaic showing the topography of the Brampton Kame Belt (dashed red line). (B) Geomorphological map of the Brampton Kame Belt (dashed black line). Sites of GPR lines and sediment sections presented in the paper: MF = Morley Farm, BF = Brampton Farm, CF = Carlatton Farm, NS = North Scales. Additional locations of relevance: BR = Brampton ridge, TT = Talkin Tarn.

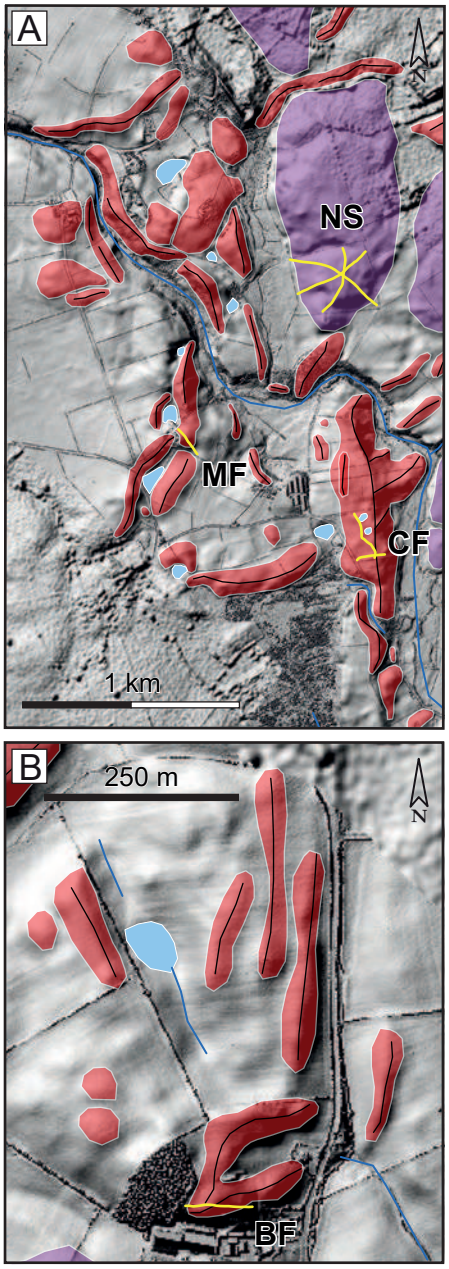

Figure 3 – Location and geomorphological context of GPR lines (in yellow) presented in this study. Underlying images are 1 m resolution DSMs. (A) Morley Farm (MF), Carlatton Farm (CF) and North Scales (NS) sites. (B) Brampton Farm (BF) site. See Fig. 2B for full geomorphological map and legend.

Radar facies	Example	Characteristics	Interpretation
RF1	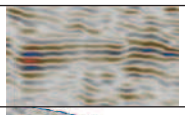	Continuous and strong sub-horizontal to wavy reflectors	Sub-horizontally bedded sands
RF2	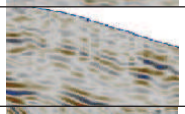	Discontinuous sub-horizontal reflectors	Gravel sheets/layers. In some cases may represent deformed sediment packages
RF3	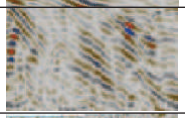	Dipping relfectors, sometimes discontinuous and often downlapping onto underlying radar surfaces	Foresets/backsets
RF4	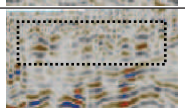	Faint sub-horizontal reflectors, typically overlying RF3 and in places mimicking underlying radar surfaces	Topsets/draped lake sediments
RF5	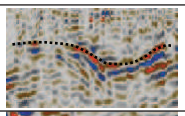	Continuous and discontinuous undulating reflectors with a hummocky upper surface mimicking underlying reflectors	Ridge-scale sedimentation (macroforms) within an ice-walled channel. In some contexts could be subaqueous fan deposits
RF6	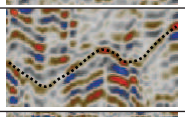	Trough-shaped features containing sub-horizontal reflectors	Channels, either continuous sedimentation within migrating system, or incised and infilled
RF7	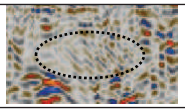	Disorganised reflectors, steeply-angled in places. Can include offset reflectors, possible evidence for faulting	Deformed sediment packages

Figure 4 – Radar facies classification used to describe and interpret the GPR profiles.

Figure 5

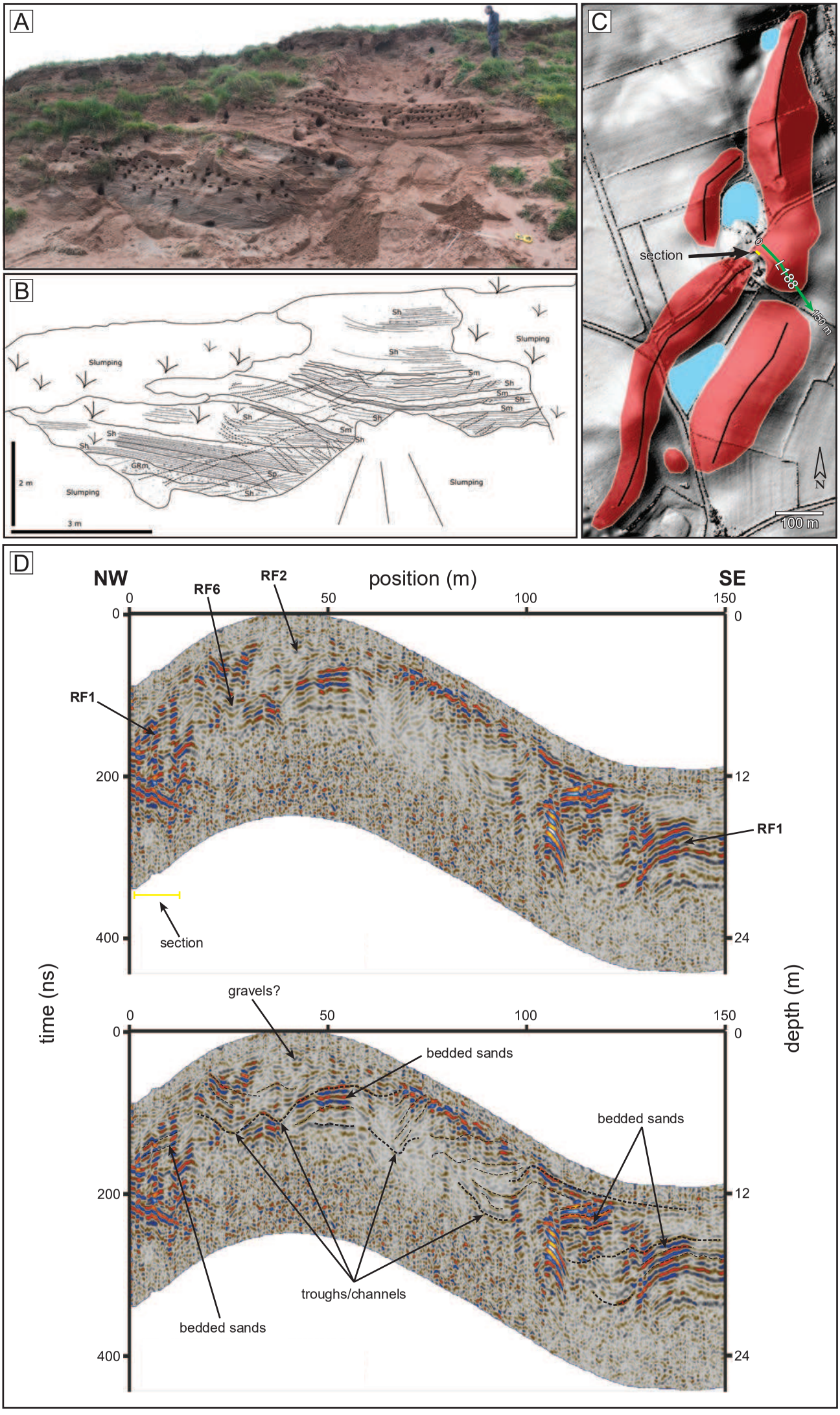

Figure 5 – Morley Farm site. (A) Section photo. (B) Sediment log. (C) DSM showing mapped ridges (in red) and depressions (in blue) with location of section (yellow line) and GPR line 188 (green arrow). (D) GPR line 188 and annotated interpretation of GPR data. See text and Fig. 4 for reference to numbered radar facies (RF). Approximate location of section in (A) and (B) is indicated by the yellow line in the top panel. See Figs. 2B and 3A for location of site.

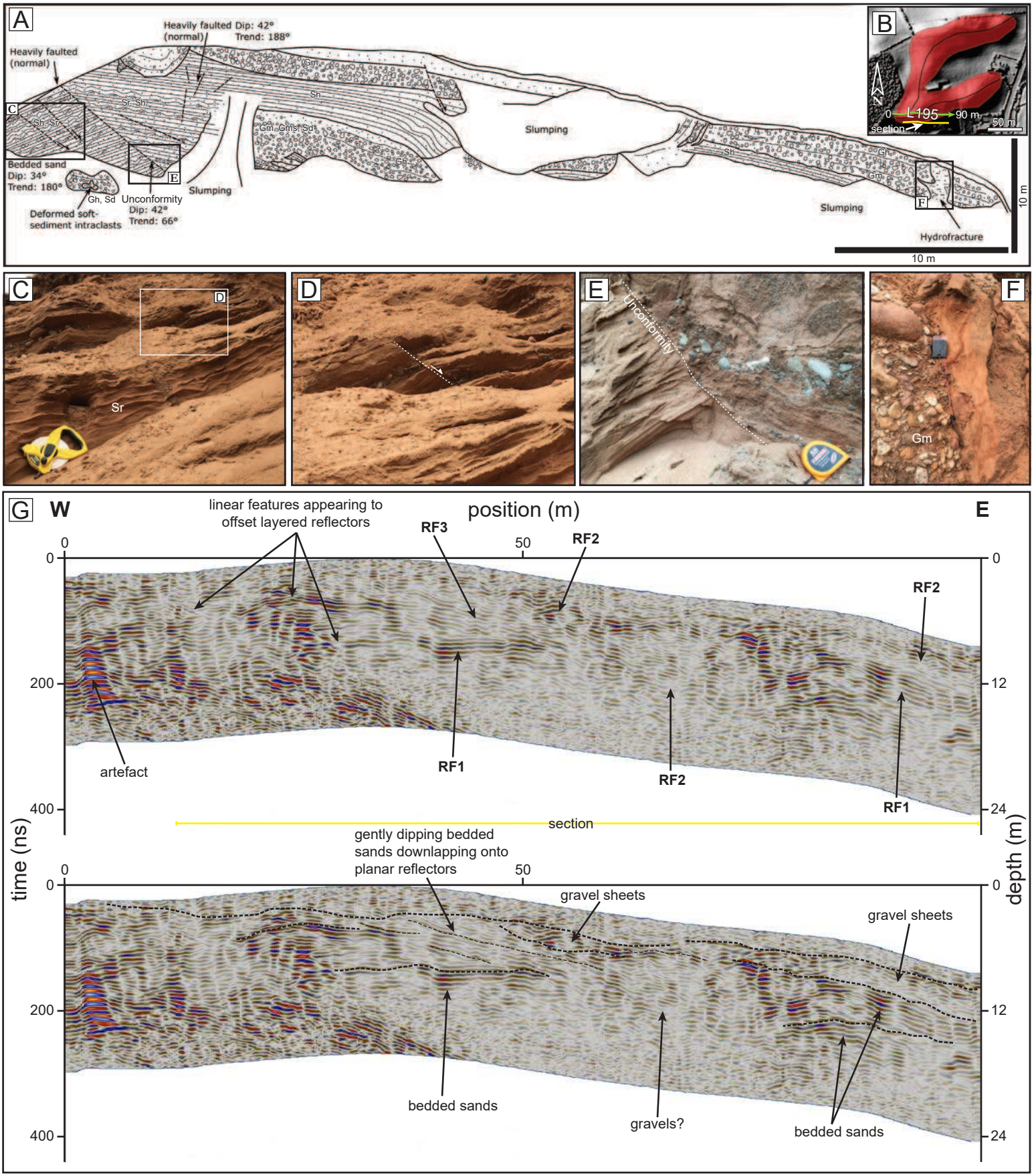

Figure 6 – Brampton Farm site. (A) Sediment log. (B) DSM showing mapped ridges (in red) and location of section (yellow line) and GPR line 195 (green arrow). (C) to (F) Photographs showing close-up of details in (A). (G) GPR line 195 and annotated interpretation of GPR data. See text and Fig. 4 for reference to numbered radar facies (RF). Approximate location of section in (A) is indicated by the yellow line in the top panel. The diagonal swipes to the west end of the section are thought to be artefacts from trees located at the edge of the field. See Figs. 2B and 3B for location of site.

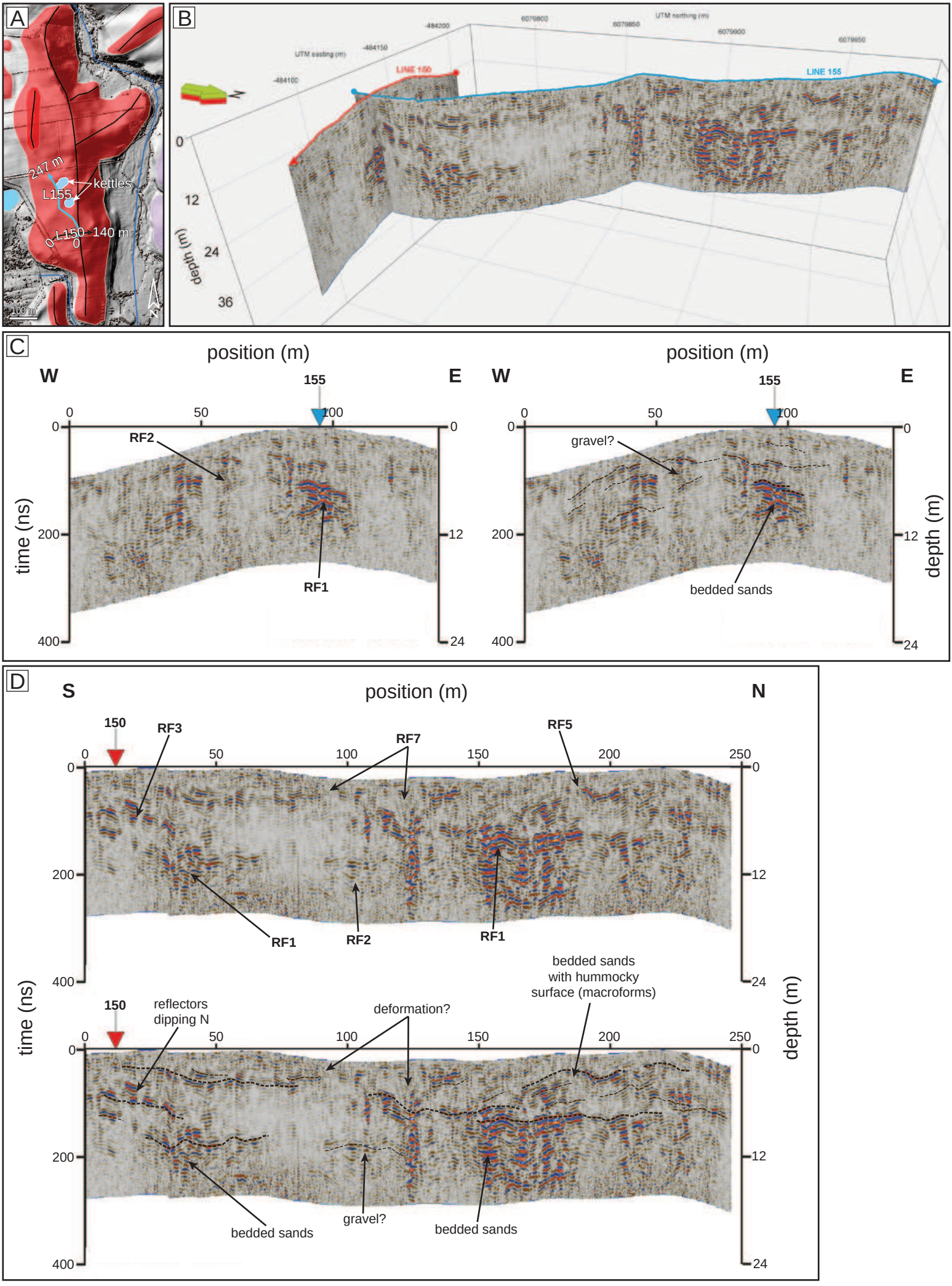
A
247 m
kettles
L155
L150
140 m
100 m
B
UTM easting (m)
UTM northing (m)
LINE 150
LINE 155
depth (m)
C
position (m)
W
E
155
RF2
RF1
gravel?
bedded sands
time (ns)
depth (m)
D
S
N
150
RF3
RF7
RF5
RF1
RF2
RF1
bedded sands
with hummocky
surface (macroforms)
reflectors
dipping N
deformation?
bedded sands
gravel?
bedded sands

Fig. 7

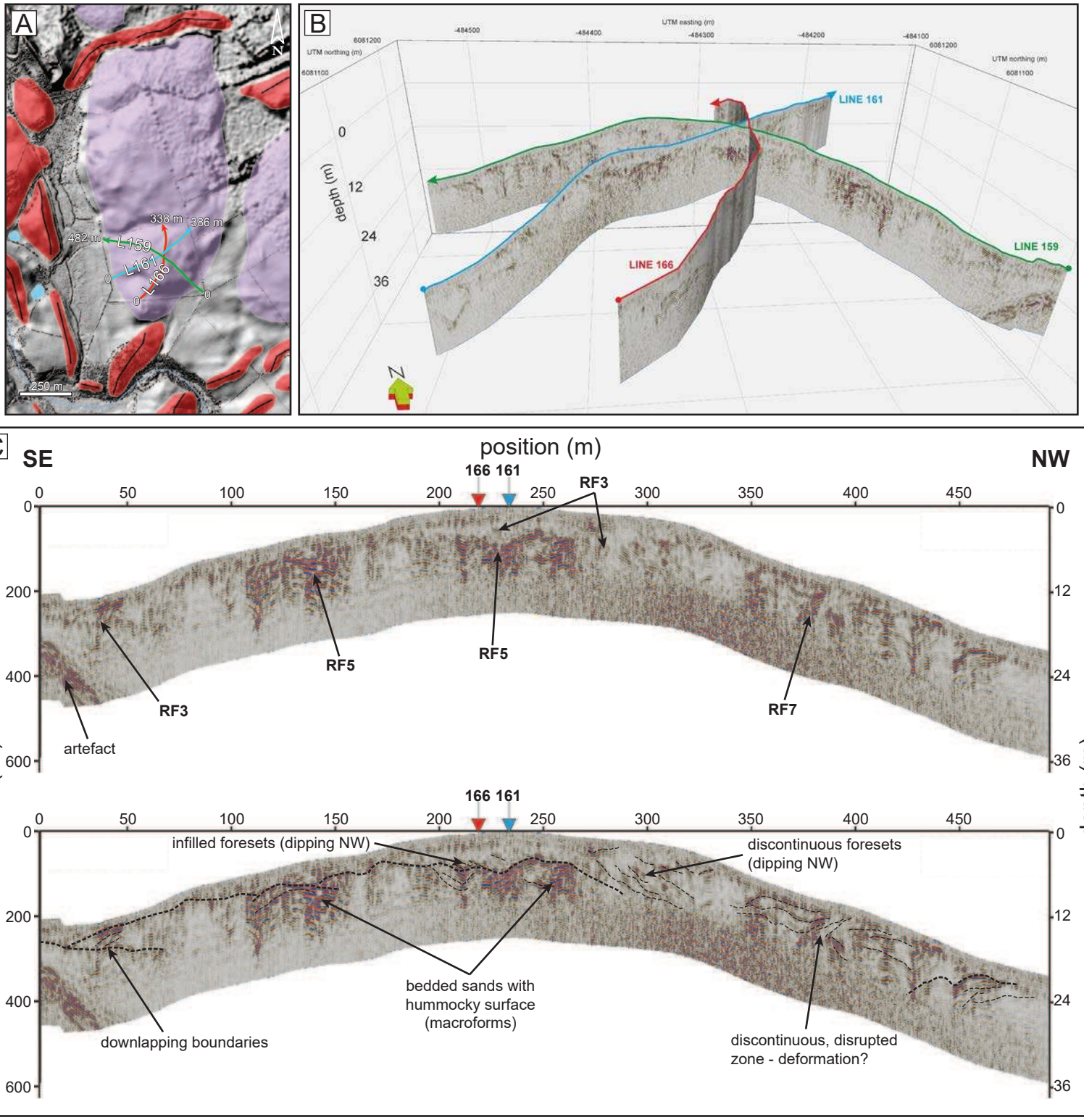

Figure 8 – GPR lines 159, 161 and 166 collected from North Scales flat-topped hill. (A) DSM showing mapped flat-topped hills (in purple), ridges (in red), depressions (in blue), and meltwater channels (blue lines) with location of GPR lines 159 (green arrow), 161 (blue arrow) and 166 (red arrow). See Figs. 2B and 3A for location of site. (B) Fence diagram of lines. (C) Line 159 and annotated interpretations. (D) Line 161 and annotated interpretations. (E) Line 166 and annotated interpretations. See text and Fig. 4 for reference to numbered radar facies (RF) in (C), (D) and (E).

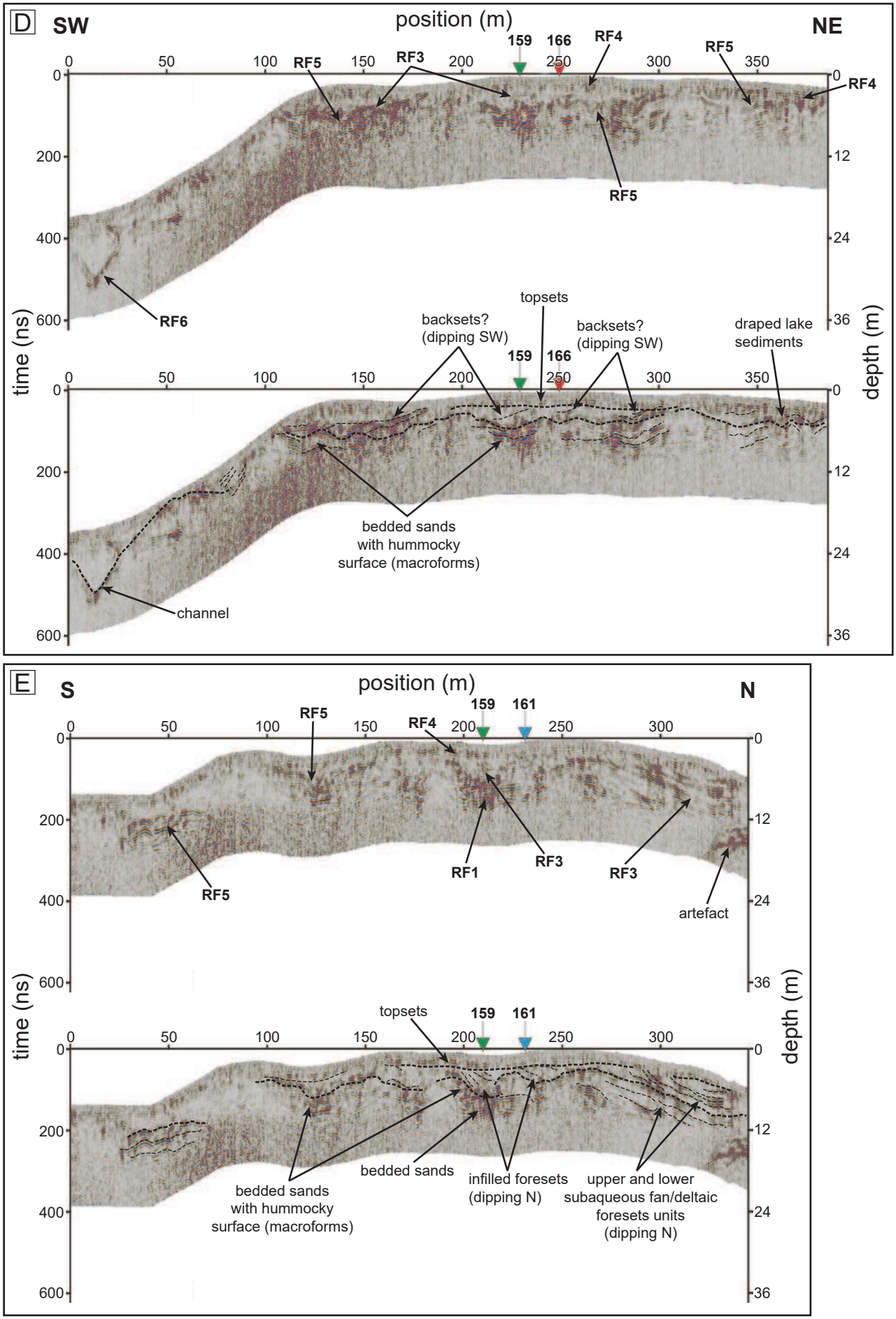

Figure 8 – continued.

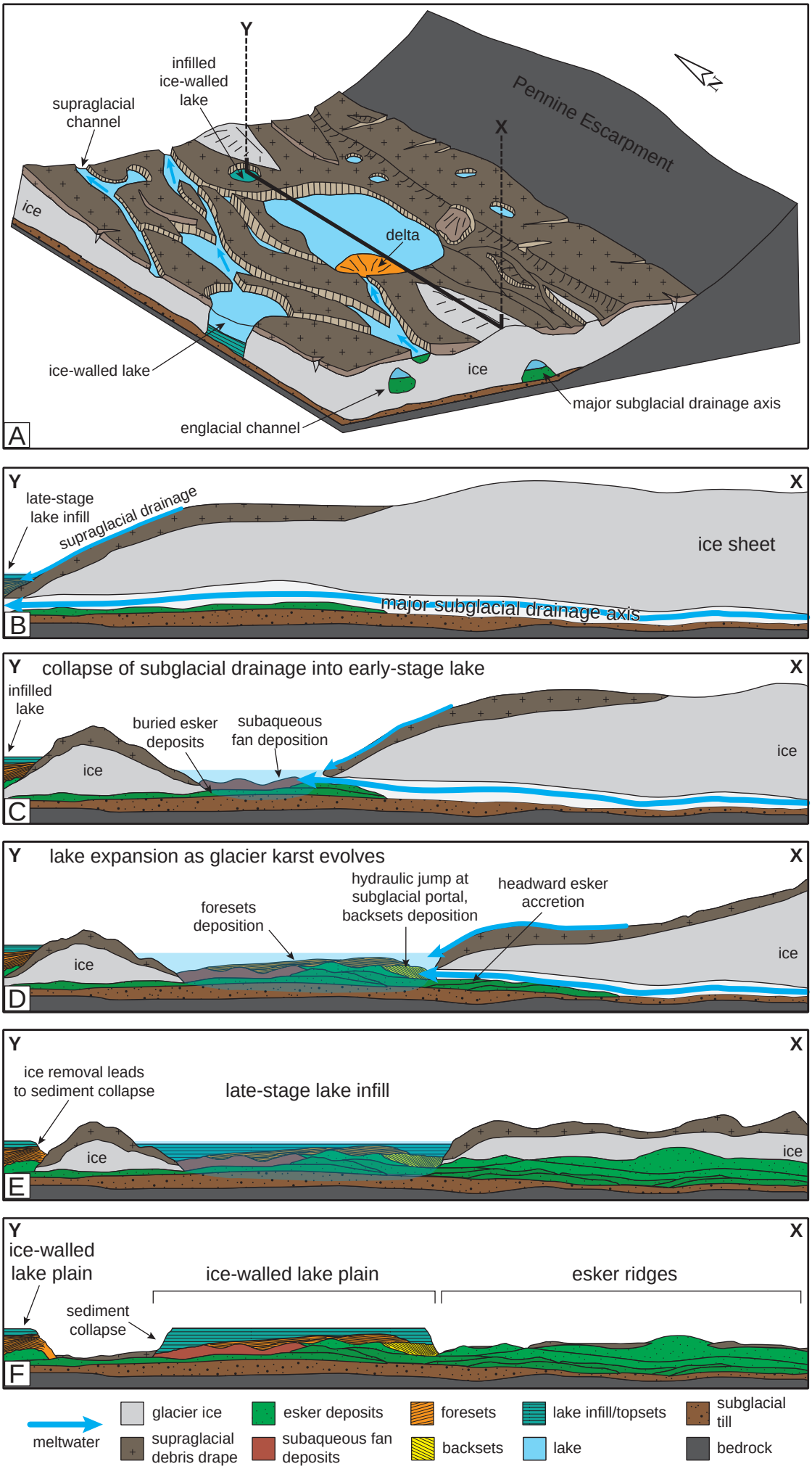
Y
infilled
ice-walled
lake
supraglacial
channel
Pennine Escarpment
X
ice
delta
ice-walled lake
ice
major subglacial drainage axis
englacial channel
A
Y
late-stage
lake infill
supraglacial drainage
X
ice sheet
major subglacial drainage axis
B
Y
collapse of subglacial drainage into early-stage lake
X
infilled
lake
buried esker
deposits
subaqueous
fan deposition
ice
ice
C
Y
lake expansion as glacier karst evolves
X
hydraulic jump at
subglacial portal,
backsets deposition
headward esker
accretion
foresets
deposition
ice
ice
D
Y
X
ice removal leads
to sediment collapse
late-stage lake infill
ice
ice
E
Y
X
ice-walled
lake plain
ice-walled lake plain
esker ridges
sediment
collapse
F
meltwater
glacier ice
supraglacial
debris drape
esker deposits
subaqueous fan
deposits
foresets
backsets
lake infill/topsets
lake
subglacial
till
bedrock

Fig. 9

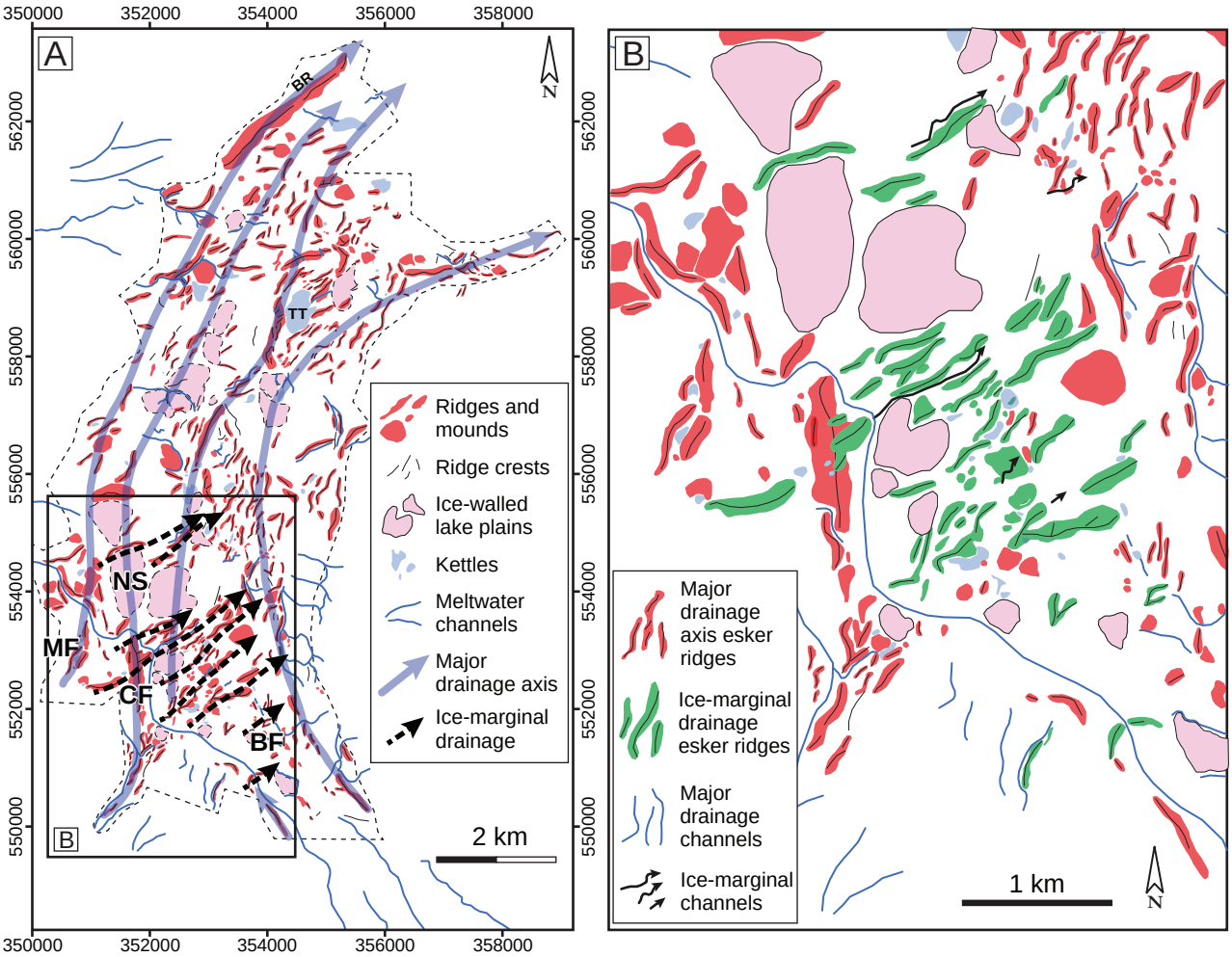
A
B
BR
TT
NS
MF
CF
BF
N
Ridges and mounds
Ridge crests
Ice-walled lake plains
Kettles
Meltwater channels
Major drainage axis
Ice-marginal drainage
2 km
Major drainage axis esker ridges
Ice-marginal drainage esker ridges
Major drainage channels
Ice-marginal channels
1 km
350000
352000
354000
356000
358000
562000
560000
558000
556000
554000
552000
550000

Fig. 10

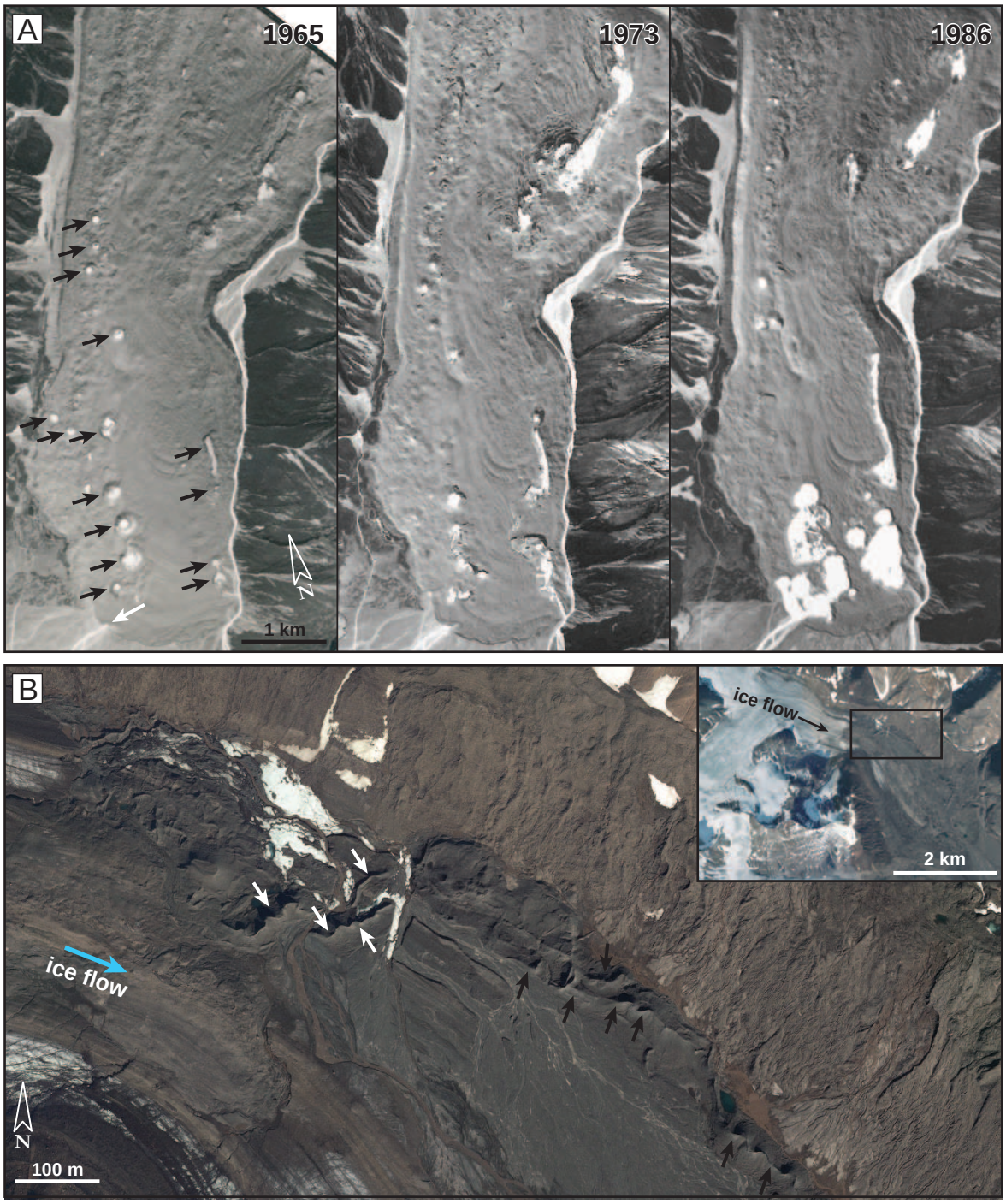

Fig. 11

Complex kame belt morphology, stratigraphy and architecture

Harold Lovell*, Stephen J. Livingstone, Clare M. Boston, Adam Booth, Robert D. Storrar and Iestyn D. Barr

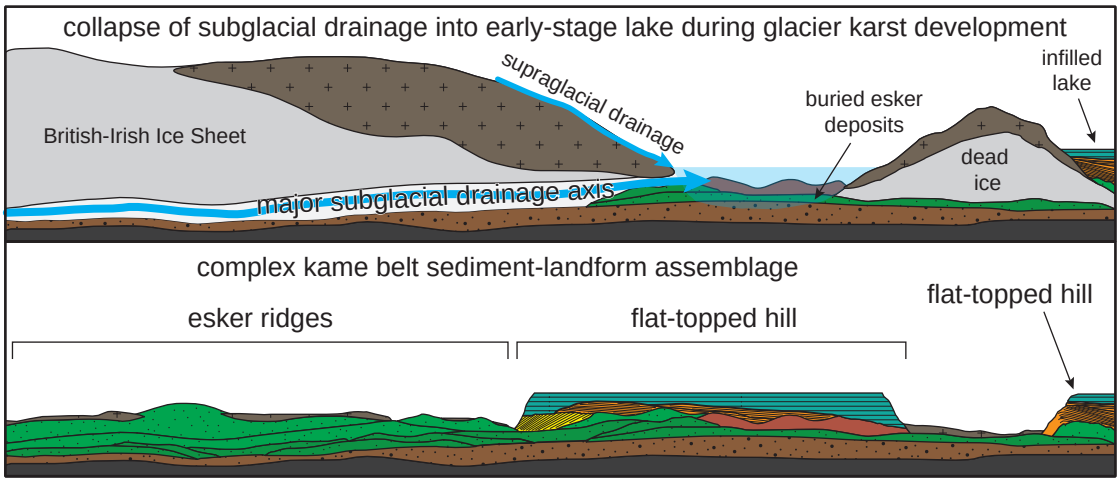

We present a combined geomorphological, sedimentological and geophysical (ground-penetrating radar) investigation of the Brampton Kame Belt, UK. These data allow us to propose a model for flat-topped hill formation as ice-walled lake-plains that evolve from the collapse of major subglacial drainage axes during ice sheet downwasting. Two styles of drainage can be identified within the kame belt: major subglacial drainage axes orientated S-N, and smaller fragmentary eskers orientated SW-NE and formed in ice-marginal positions during south-eastwards retreat.

Graphical abstract